Magnetic phase diagram of the ferromagnetically stacked triangular XY antiferromagnet: A finite-size scaling study

M. L. Plumer, A. Mailhot,* and A. Caillé
Centre de Recherche en Physique du Solide et Département de Physique
Université de Sherbrooke, Sherbrooke, Québec, Canada J1K 2R1
(Received 9 December 1993)

Histogram Monte Carlo simulation results are presented for the magnetic-field–temperature phase diagram of the XY model on a stacked triangular lattice with antiferromagnetic intraplane and ferromagnetic interplane interactions. Finite-size scaling results at the various transition boundaries are consistent with expectations based on symmetry arguments. Although a molecular-field treatment of the Hamiltonian fails to reproduce the correct structure for the phase diagram, it is demonstrated that a phenomenological Landau-type free-energy model contains all the essential features. These results serve to complement and extend our earlier work [Phys. Rev. B **48**, 3840 (1993)].

I. INTRODUCTION

Although finite-size scaling studies of critical phenomena based on Monte Carlo histogram (MCH) data[1] for unfrustrated systems have proven highly effective in the estimation of critical exponents[2] and in the determination of weakly first-order transitions,[3] corresponding studies of possibly more interesting frustrated lattices have proven more demanding.[4–8] The utility of this approach in examining the critical properties of the variety of phase transitions which occur under the influence of an applied magnetic field in the ferromagnetically stacked triangular XY antiferromagnet is demonstrated here. The Hamiltonian is written as

$$\mathcal{H} = J_{\|} \sum_{\langle ij \rangle} \mathbf{S}_i \cdot \mathbf{S}_j + J_{\perp} \sum_{\langle kl \rangle} \mathbf{S}_k \cdot \mathbf{S}_l - H \sum_i S_{xi}, \quad (1)$$

where the spins lie in the basal plane, $J_{\|} < 0$ is the ferromagnetic interplane interaction, $J_{\perp} > 0$ indicates the antiferromagnetic coupling which is frustrated for the triangular geometry, $\langle i,j \rangle$ and $\langle k,l \rangle$ represent near-neighbor sums along the hexagonal c axis and in the basal plane, respectively, and the field is applied in the basal-plane direction x. The general structure of the phase diagram is shown in Fig. 1 of our earlier work[7] (hereafter referred to as I). Phases are labeled by the nonzero components of the (complex) spin polarization vector $\mathbf{S} = \mathbf{S}_a + i\mathbf{S}_b$. The Néel transition at zero field is to the well-known helically polarized 120° spin structure ($S_{ax} = S_{by}$). Indicated in the figure are the elliptically polarized phase 7, linear phases 6 and 9, as well as the paramagnetic state 1. Phase 6 is of particular interest as it has the symmetry of the three-state Potts model and should exhibit a first-order transition to the paramagnetic state. This was confirmed by extensive finite-size scaling of the extrema in various thermodynamic functions which occur at the 1-6 phase boundary for magnetic field strengths $H = 0.7$ and $H = 1.5$. Data for $H = 0.7$ can be found in I. In addition to presenting the corresponding MCH data at $H = 1.5$, finite-size scaling results are given here for the other three transition lines.

It is of interest to note that Lee *et al.*[9] examined the XY antiferromagnet on a triangular lattice (unstacked) in an applied magnetic field. At H=0, the transition shows Kosterlitz-Thouless (KT) behavior but the field breaks rotational symmetry and transitions involving true long-range spin order can occur. The resulting phase diagram in this two-dimensional (2D) case is very similar to that of the present model. Using traditional finite-size scaling of their MC data, these authors reported that the 1-6 transition belongs to the 2D three-state Potts universality class, but that the other transition lines exhibited nonuniversal critical behavior; different exponents were found for different points on a transition line. We find that this latter conclusion is somewhat surprising but may be due to KT-like excitations in some cases. The possibility always exists that the MC data were not sufficiently accurate to distinguish among the variety of possibilities.

Before discussing our own MCH data for the 3D model, it is useful to examine the results of a mean-field analysis based on the Landau theory of phase transitions.

II. MEAN-FIELD THEORY

Mean-field analyses of magnetic phase diagrams based on Landau-type free energies for frustrated spin systems have proven to be quite successful in reproducing the essential features of both MC and experimental results.[8] (A notable exception is the XY model on a stacked triangular lattice, with both $J_{\|}, J_{\perp} > 0$, in the quasi-2D case[10] where $J_{\|} \ll J_{\perp}$.) It was previously demonstrated for the 2D version of the present model that a molecular-field treatment of the Hamiltonian (1) yields a phase diagram with phase 6 absent.[11] Identical results are expected for the 3D model under consideration here. It is shown

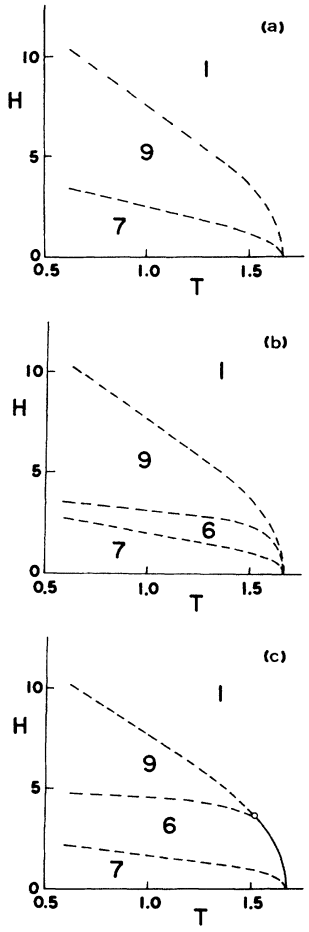

FIG. 1. Mean-field results for the phase diagram, where (a) is based on a free energy derived from molecular-field theory, (b) is from the phenomenological Landau free energy (3) with all parameters as in (a) except $B_4 = 1$, and (c) is from the same model as (b) but with $B_4 = 0.1$.

below, however, that the phenomenological Landau approach can capture all of the essential features of the phase diagram. Such a treatment is also useful in understanding analytically the interactions which are responsible for stabilizing each phase. In addition, an examination of such a free energy (which has the same structure as an appropriate Landau-Ginzburg-Wilson Hamiltonian), together with symmetry arguments, is useful in determining expectations regarding the critical behavior of the various transition lines.

Following the method outlined in Ref. 12, the free energy is expanded to fourth order in the spin density

$$\mathbf{s}(\mathbf{r}) = \mathbf{m} + \mathbf{S}e^{i\mathbf{Q}\cdot\mathbf{r}} + \mathbf{S}^* e^{-i\mathbf{Q}\cdot\mathbf{r}}, \tag{2}$$

where $\mathbf{m}$ is the uniform component induced by the magnetic field and $\mathbf{Q}$ is the wave vector. The result can be written as

$$\begin{aligned} F = {} & A_Q S^2 + \tfrac{1}{2}A_0' m^2 + B_1 S^4 + \tfrac{1}{2}B_2 \mid \mathbf{S}\cdot\mathbf{S} \mid^2 \\ & + \tfrac{1}{4}B_3 m^4 + 2B_4 \mid \mathbf{m}\cdot\mathbf{S} \mid^2 + B_5 m^2 S^2 \\ & + B_6[(\mathbf{m}\cdot\mathbf{S})(\mathbf{S}\cdot\mathbf{S}) + \text{c.c.}] \\ & + \cdots - \mathbf{m}\cdot\mathbf{H}, \end{aligned} \tag{3}$$

where $A_Q = a(T - T_Q)$ and $A_0' = a(T - T_0')$. This expression is identical to that used in our analysis of the magnetic phase diagram for the case of antiferromagnetic interplane coupling[13] *except* for the additional term B_6. As emphasized in I, this term *cubic* in $\mathbf{S}$ occurs since the ordering wave vector satisfies the relation $3\mathbf{Q} = \mathbf{G}$, where $\mathbf{G}$ is a reciprocal lattice vector. The cubic term is responsible for the stability of the three-state Potts phase 6. It is important to note that from symmetry arguments alone, each of the fourth-order coefficients B_i in (3) is independent since each corresponding term is an independent invariant with respect to the relevant symmetry operations.

A free energy identical in structure to (3) may also be *derived* from a molecular-field treatment of the Hamiltonian (1).[14] In this case, all the fourth-order coefficients are the same and given by $B_i = bT$, where for classical spins $b = \frac{9}{5}$. Since the Landau expansion is applicable only in regions where S is small, the approximation $B_i \simeq bT_N$ is usually made. In addition, the molecular-field treatment yields $a = 3$, as well as

$$T_Q = 2(-J_{\parallel} + 3J_{\perp})/a, \quad T_0' = -2(J_{\parallel} + 3J_{\perp})/a. \tag{4}$$

Thus, the exchange constants are the only parameters which appear in this theory.

Figure 1(a) shows the resulting phase diagram from an analysis of the free energy from molecular-field theory expanded to sixth order in $\mathbf{s}$ using $J_{\parallel} = -1$, $J_{\perp} = 1$ and $\mathbf{H}\|\hat{\mathbf{x}}$. It is seen to have the same structure as the mean-field result in Ref. 11. The three-state Potts phase 6 does not appear. An analysis of the free energy reveals that this state is somewhat accidentally excluded. This conclusion is demonstrated by results from the more general phenomenological model. Analysis was made using the same parameter values as in the molecular-field theory, except that one of the fourth-order coefficients B_i was made to be different from bT. Results for the cases $B_4 \equiv 1$ and 0.1 are shown in Figs. 1(b) and 1(c), respectively. Phase 6 now appears. The correct structure of the true phase diagram (Fig. 1 of I) is reproduced by the smaller value of B_4. Similar results occur if only B_2 or B_3 is set to be different from the other B_i. It seems that some effects of critical fluctuations not accounted for within mean-field theory can be mimicked (by renormalization of the coefficients) in the more general phenomenological model in this case.

The stability of each state in the phase diagram can be understood by examining the terms in (3) with the assumption $B_i > 0$. At zero applied field ($m = 0$), the B_2 term is minimized with $\mathbf{S}\cdot\mathbf{S} = 0$. This is achieved by a helical polarization $S_{ax} = S_{by}$. At low temperatures and low values of the applied field, the B_4 term, which favors a configuration $\mathbf{S}\perp\mathbf{m}$, distorts the helix into an ellipse (phase 7), $S_{ax} \neq S_{by}$. At higher temperatures and low field values, the B_6-term dominates and favors phase 6 with a configuration $\mathbf{S}\|\mathbf{m}$. The high-field phase 9 is a result of both B_4- and B_6-type interactions which favor a linear polarization.

This analysis allows some predictions to be made regarding the nature of the various phase transition lines.

The 1-6 line should be first order due to the relevance of the cubic term B_6, as confirmed in I. (We note, however, that mean-field theory would also suggest the same behavior in 2D. In fact, this transition belongs to the 2D three-state Potts universality class.) A continuous 1-9 transition is the result of the mean-field analysis despite the nonzero value of the Potts variable S_{ax}. A first-order transition does not occur in this case because, as discussed in I, the B_6 term effectively disappears at the paramagnetic boundary line at some power of S greater than 3. It is not clear what the effects of critical fluctuations will be regarding this scenario. If the transition is continuous, it should belong to the XY universality class since both S_{ax} and S_{ay} are involved. The remaining two transition lines, 6-7 and 6-9, should both belong to the Ising universality class as only a single component of **S** is involved in each case. A purpose of the finite-size scaling analysis described below is to test these predictions.

III. FINITE-SIZE SCALING

The analysis of MC-generated histograms used here to determine finite-size scaling behavior is described in I. In most cases, scaling was performed on the extrema of a variety of thermodynamic functions, including the specific heat C, susceptibility χ, energy cumulant $U(T) = 1 - \frac{1}{3}\langle E^4\rangle/\langle E^2\rangle^2$, and the logarithmic derivative of the order parameter M, which is equivalent to $V(T) = \langle ME\rangle/\langle M\rangle - \langle E\rangle$. The energy cumulant exhibits a minimum near T_N, which achieves the value $U^* = \frac{2}{3}$ in the limit $L \to \infty$ for a continuous transition, whereas $U^* < \frac{2}{3}$ is expected in the case of a first-order transition. The thermodynamic quantities should display volume-dependent scaling, L^3, in the case of a first-order transition (except for M), or scaling as L^x, where x is a ratio of critical exponents, in the case of a continuous transition. Finite-size scaling results for the order parameter, evaluated at the estimated critical temperature, are presented only for the 1-9 transition. For reasons unknown to us, it appeared that the values of L used here were to small to obtain reliable results for this quantity in the other cases where a continuous transition was expected. Partly due to the relatively large fluctuations in the MCH data, a general feature of frustrated systems,[8] the approach taken in this work is to simply determine if the results are consistent with the expectations and possibilities outlined above: Scaling was performed with assumed exponent values. This method of presenting data was also used in I, as well as in Refs. 5 and 6, and is useful in cases where the true critical behavior may be revealed only at larger lattice sizes. The alternate approach of presenting data in the form of log-log plots is more appropriate in cases where very reliable statistics are available and finite-size correction terms to simple L^x behavior should be negligible.

Simulations were performed on the Hamiltonian (1) with $J_{\|} = -1$ and $J_{\perp} = 1$ using periodic boundary conditions on $L \times L \times L$ lattices. In most cases, a random initial spin configuration was used and thermodynamic averages were estimated after discarding the first 2×10^5 MC

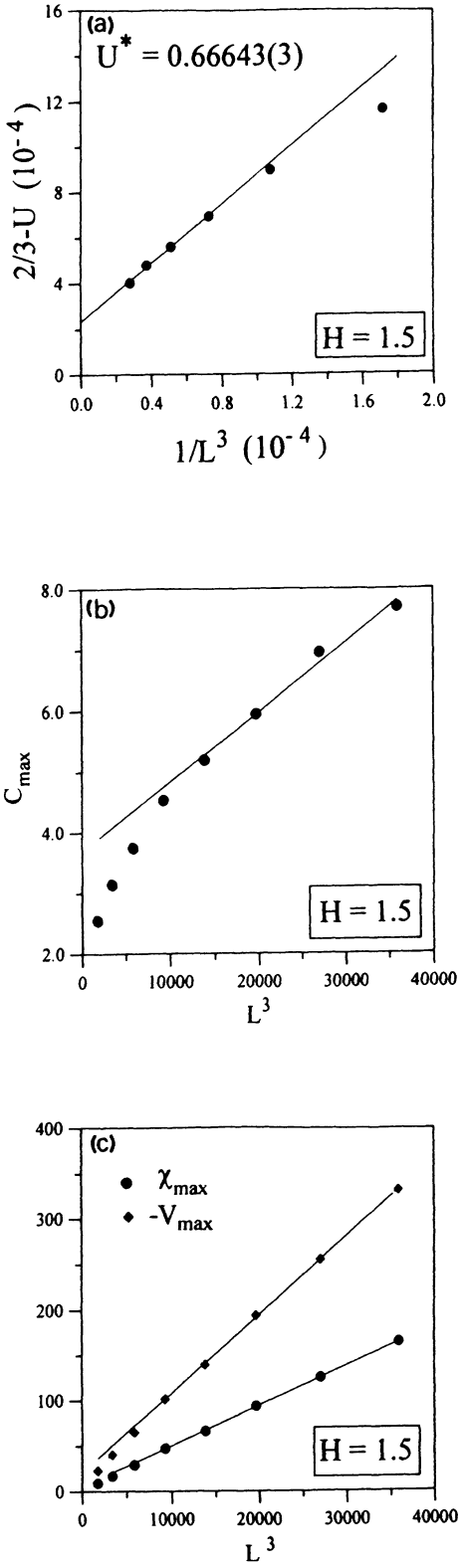

FIG. 2. Finite-size scaling of extrema for the 1-6 transition at $H = 1.5$ near $T_c \simeq 1.522$ with the assumption of volume dependence. (a) shows the energy cumulant, where values for $L = 12$ and 15 have been omitted to allow for an expanded scale. All results for L=12–33 are shown in (b) and (c) for the specific heat, susceptibility, and logarithmic derivative of the order parameter.

steps for thermalization. In other cases, the final, well-thermalized, configuration of a previous run was used for the initial spin directions. Further details are given in the following sections which describe the results of finite-size scaling at each phase-boundary line.

A. H=1.5: 1-6 transition

Results of the histogram analysis at $H = 1.5$ for the 1-6 phase boundary are also discussed briefly in I. Simulations were performed on lattices $L = 12$–33 with 1–2.6×10^6 MC steps used for thermal averaging. The increased number of MC steps for larger lattices was used in an effort to account for an expected increase in the correlation time. Histograms were made at $T = 1.52$ and $T = 1.523$ and the critical temperature was estimated to be $T_c = 1.522(2)$ from the finite-size dependence of the various thermodynamic extrema. The results shown in Fig. 2 demonstrate that the expected volume dependence of a first-order transition may not be evident at smaller values of L. This aspect of MC simulations has only recently been emphasized.[3,6] The extrapolated value of the energy cumulant [Fig. 2(a)] is close to the value expected of a continuous transition, $\frac{2}{3}$, indicating that it is only weakly first order. This conclusion is corroborated by the estimated latent heat given in I.

B. H=0.7: 6-7 transition

The 6-7 boundary is expected to be a line of continuous transitions belonging to the Ising universality class. MC histograms were made for L=12–30 at several temperatures between $T = 1.40$ and $T = 1.45$ using 1–3×10^6 steps for averaging. The transition temperature was estimated to be $T_c = 1.425(4)$. Much difficulty was experienced in locating extrema in the thermodynamic quantities for $L = 12$ and these data were not used in the finite-size scaling analysis. Several runs using the larger lattices exhibited widely varying results, indicating that critical fluctuations are significant at this transition (possibly due to the proximity of the paramagnetic state). For example, it was not possible to obtain reliable results for the order parameter. Figure 3(a) shows a logarithmic plot of the energy cumulant. The extrapolated value $U^* = 0.666\,665(4)$ suggests that the transition is indeed continuous. The slope $-2.9(1)$ is close to -3, as expected for continuous transitions if the exponent ratio α/ν is small,[15] as in the present case. Finite-size scaling of the other thermodynamic quantities shown in Fig. 3 was made with the assumption of Ising critical exponents.[5] As in the case of Fig. 2, these results suggest that the true critical behavior is revealed only at larger lattice sizes (especially the data for $V_{\max}$). Scaling with the assumption of volume dependence gave results which could not be fit to a straight line.

C. H=2.7: 6-9 transition

The anticipated difficulty in obtaining reliable estimates for the location of extrema in the thermodynamic quantities as a function of temperature at the 6-9 transition was realized. This was due to the near zero slope of this boundary line in the H-T plane so that large fluctu-

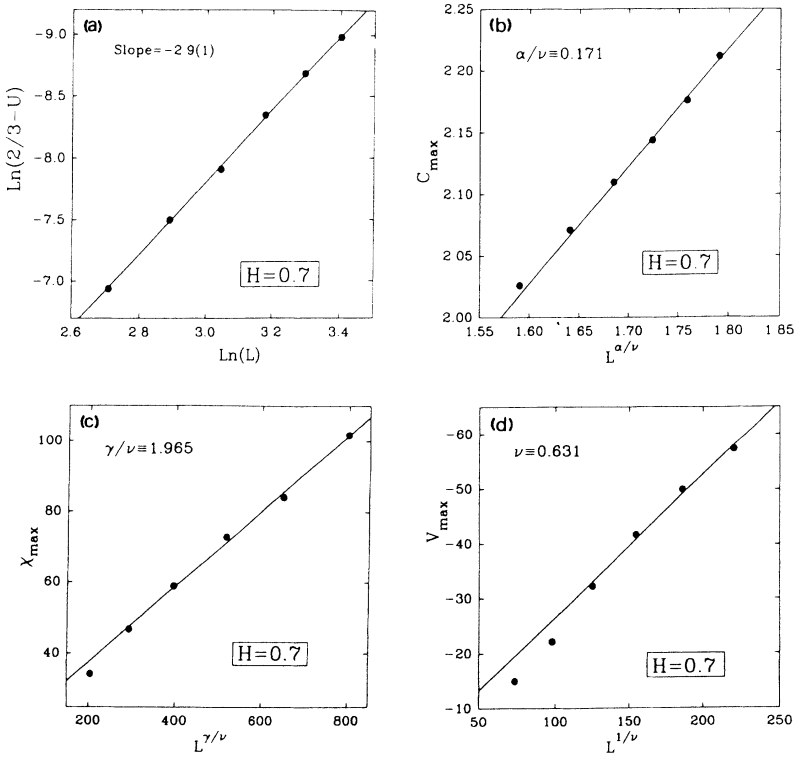

FIG. 3. Finite-size scaling of extrema for the 6-7 transition at $H = 0.7$ near $T_c \simeq 1.425$ with the assumption of Ising univerality using data from lattices $L = 15$–30.

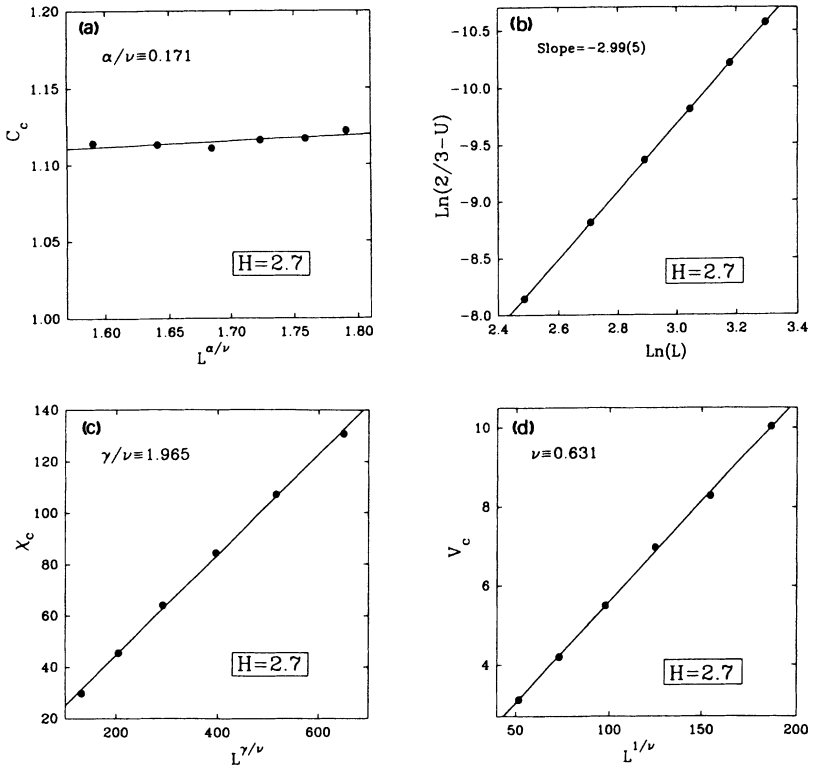

FIG. 4. Finite-size scaling results for the 6-9 transition at $H = 2.7$ of thermodynamic functions evaluated *at* $T_c \simeq 1.23$ with the assumption of Ising univerality using data from lattices $L = 12$–27.

ations between the two phases occurred. (A more suitable, but a more memory- and time-consuming, approach would have been to obtain extrema as a function of magnetic field from the histograms.[1]) For this reason, finite-size scaling was performed *at* the (crudely) estimated critical temperature. Smaller lattice sizes, $L = 12$–27, were chosen in order to minimize the effect of an error in the estimated T_c. 2–7 × 10^6 MC steps were used to create histograms at a number of temperatures between $T = 1.20$ and 1.28. Scaling consistent with the anticipated Ising universality, as shown in Fig. 4, was found by assuming a critical temperature $T_c = 1.23(1)$. Note

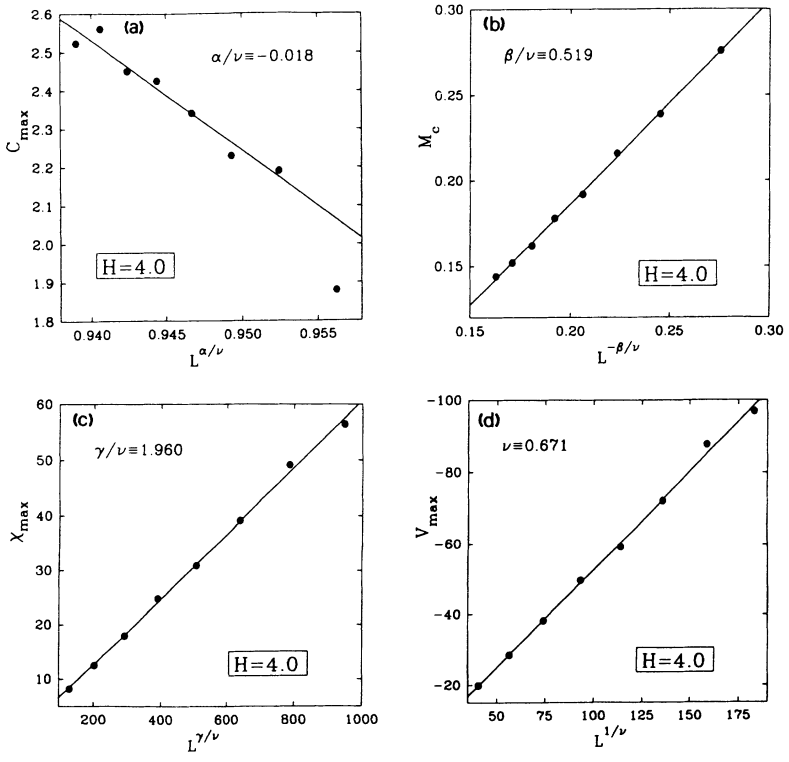

FIG. 5. Finite-size scaling of extrema for the 1-9 transition at $H = 4.0$ near $T_c \simeq 1.423$ with the assumption of XY univerality using data from lattices L=12–33.

that the scale of Fig. 4(a) for the specific heat is approximately the same as used in Fig. 3(b) and reflects the very small slope of the fitted line. Our MCH results for the order parameter were again found not to be reliable for this transition. The extrapolated value of the energy cumulant, $U^* = 0.666\,666\,8(8)$, clearly indicates that the transition is continuous. As in the previous case, the slope $-2.99(5)$ of Fig. 4(b) is consistent with a small value for α/ν.

D. H=4.0: 1-9 transition

Although the 1-9 transition is expected to belong to the XY universality class within mean-field theory, the not unlikely possibility exists that the cubic term in the free energy becomes relevant when critical fluctuations are included. Histogram data were taken at $T = 1.42$ and $T = 1.44$ on lattice sizes $L = 12$–33 with 1–3×10^6 steps for averaging. Volume-dependent scaling was not observed in the extrema of thermodynamic functions. Further support for the continuous nature of this transition comes from the extrapolated value $U^* = 0.666\,666\,4(8)$, where the energy-cumulant scaling exponent was found to be $-2.8(2)$. Finite-size scaling consistent with XY universality is shown in Fig. 5, including the order parameter evaluated at the estimated critical temperature $T_c = 1.423(4)$.

IV. CONCLUSIONS

This work on the phase diagram of ferromagnetically coupled antiferromagnetic XY triangular layers contains two results of importance. The first is that although molecular-field theory fails, a more general phenomenological model is capable of capturing all the essential features. This mean-field model also allows specific predictions to be made regarding the expected critical behavior. Second, the histogram Monte Carlo method has been demonstrated to be useful in verifying this anticipated criticality through finite-size scaling of thermodynamic functions. Relatively large fluctuations observed in the MC data are attributed to the frustration inherent in the triangular geometry. These results serve to complement and extend our earlier work,[7] as well as that of Lee *et al.*[9] who studied the corresponding two-dimensional system. Although these authors suggest nonuniversal critical behavior on all transition lines, except the 1-6 boundary, in the 2D case, our analysis suggests that only the 1-9 transition should exhibit XY symmetry and the consequent KT-like excitations associated with such nonuniversality. It is of interest to perform histogram MC simulations on the 2D system to examine these issues further. As mentioned in I, a good experimental candidate for the present 3D model is $La_2Co_{1.7}$.[16]

ACKNOWLEDGMENTS

This work was supported by NSERC of Canada and FCAR du Québec.

* Present address: INRS-EAU, 2800 rue Einstein, C.P. 7500, Sainte-Foy, Québec, Canada G1V 4C7.

[1] A.M. Ferrenberg and R.H. Swendsen, Phys. Rev. Lett. **61**, 2635 (1988); **63**, 1195 (1989); Comput. Phys. **3** (5), 101 (1989).

[2] P. Peczak, A.M. Ferrenberg, and D.P. Landau, Phys. Rev. B **43**, 6087 (1991); A.M. Ferrenberg and D.P. Landau, *ibid.* **44**, 5081 (1991); C. Holm and W. Janke, *ibid.* **48**, 936 (1993); K. Chen, A.M. Ferrenberg, and D.P. Landau, *ibid.* **48**, 3249 (1993).

[3] P. Peczak and D.P. Landau, Phys. Rev. B **39**, 11932 (1989); J. Lee and J.M. Kosterlitz, *ibid.* **43**, 3265 (1991); K. Binder *et al.*, Int. J. Mod. Phys. C **3**, 1025 (1992); K. Vollmayr, J.D. Reger, M. Scheucher, and K. Binder, Z. Phys. B **91**, 113 (1993); A. Billoire, T. Neuhaus, and B. Berg, Nucl. Phys. **B396**, 779 (1993); W. Janke, Phys. Rev. B **47**, 14757 (1993).

[4] J.N. Reimers, J.E. Greedan, and M. Björgvinsson, Phys. Rev. B **45**, 7295 (1992); A. Bunker, B.D. Gaulin, and C. Kallin, *ibid.* **48** (1993); A. Mailhot, M.L. Plumer, and A. Caillé, *ibid.* **48** (1993); T. Bhattacharya, A. Billoire, R. Lacaze, and Th. Jolicoeur, J. Phys. I (France) **4**, 122 (1994); D. Loison and H.T. Diep (unpublished); A. Mailhot *et al.* (unpublished).

[5] M.L. Plumer, A. Mailhot, R. Ducharme, A. Caillé, and H.T. Diep, Phys. Rev. B **47**, 14312 (1993).

[6] A. Mailhot and M.L. Plumer, Phys. Rev. B **48**, 9881 (1993).

[7] M.L. Plumer, A. Mailhot, and A. Caillé, Phys. Rev. B **48**, 3840 (1993). There is an error in the first paragraph of this work: Bhattacharya *et al.* have reestimated critical-exponent values which support the proposal by Kawamura of a new chiral universality class, and *not* $O(4)$ universality as stated in an earlier version.

[8] M.L. Plumer and A. Caillé, J. Appl. Phys. **70**, 5961 (1991); M.L. Plumer, A. Caillé, A. Mailhot, and H.T. Diep, in *Magnetic Systems with Competing Interactions*, edited by H.T. Diep (World Scientific, Singapore, in press).

[9] D.H. Lee, J.D. Joannopoulos, J.W. Negele, and D.P. Landau, Phys. Rev. Lett. **52**, 433 (1984); Phys. Rev. B **33**, 450 (1986).

[10] M.L. Plumer and A. Caillé, J. Appl. Phys. **69**, 6161 (1991).

[11] D.H. Lee *et al.*, Phys. Rev. B **29**, 2680 (1984).

[12] See, for example, M.L. Plumer and A. Caillé, Phys. Rev. B **37**, 7712 (1988).

[13] M.L. Plumer and A. Caillé, Phys. Rev. B **41**, 2543 (1990).

[14] M.L. Plumer, Phys. Rev. B **44**, 12376 (1991).

[15] M.S.S. Challa, D.P. Landau, and K. Binder, Phys. Rev. B **34**, 1841 (1986).

[16] D. Gignoux *et al.*, Physica B **130**, 3761 (1985).